A Dual-Band Dual-Polarized Slot Antennas Using CCLL-Inspired Metamaterial

Ali Jafargholi[1], and Amir Jafargholi[1, 2]
[1] Electromagnetic and Antenna Lab., Amirkabir University of Technology, 424 Hafez Ave., P.O. Box 15875-4413, Tehran, Iran
[2] Department of Energy Engineering and Physics, Amirkabir University of Technology, P.O. Box: 15875-4413, Tehran, Iran
E-mail: jafargholi@ieee.org (Corresponding author)

ABSTRACT:
This paper presents a compact printed dual-band dual-polarized slot antenna. The antenna is comprised of three main sections: coupled-fed, two cells of complementary capacitively-loaded loop-inspired metamaterial (CCLL-MTMs), and a slot with an overall size of 29.4×39.2 mm^2. It is shown that the CCLL-MTM structure exhibits a magneto-dielectric behavior with an effective low-frequency epsilon-negative (ENG) medium. The effective ENG material leads to a miniature printed slot antenna and a low-frequency band of 1900 MHz has been achieved. At the higher frequencies, it behaves as a magnetic material, which helps to match the antenna through a broadband frequency range. An operating band of 4750 to 5730 MHz is observed. The electric field of resonating CCLL-MTM cells and the original slot are perpendiculars, thus each band supports only a single horizontal/vertical polarization. In order to validate the simulation results, a prototype of the antenna is fabricated and tested. Good agreement between the simulation and measurement results is obtained.

KEYWORDS: Dual-band, dual-polarization, metamaterials, miniaturization, microstrip slot antenna, new long-term evolution (LTE)

1. INTRODUCTION

The increasing demands on compact multifunctional devices have necessitated the development of multi-frequency printed antennas that can be integrated into familiar devices such as tablets and laptop computers. Nowadays, the new long-term evolution (LTE) band in 4G wireless communication has attracted consideration due to a greater amount and higher speed of transmission. The typical difficulties encountered in designing compact antennas include narrow bandwidth and low radiation efficiency [1], [2]. Introducing metamaterials (MTMs) opened very interesting possibilities for the improvement of antenna and microwave components. Researchers have demonstrated metamaterial to improve antenna performance, including antennas on epsilon-near-zero (ENZ) substrate [3], composite right/left-handed (CRLH) structures [4], [5], covering the radiating parts or filling the antenna volume [6], the use of magneto-dielectric materials and metasurfaces [7], loading with a concentric pair of double-positive (DPS) and double-negative (DNG) materials [8], and DPS/mu-negative (MNG) materials [9], and near-field resonant parasitic element [10].

The capacitively-loaded loop (CLL) MTM, first introduced by Ziolkowski in [11], have found various applications in antenna engineering [12]-[16]. Thanks to the magnetic behavior of a complementary CLL-MTM (CCLL-MTM), recently the authors proposed an efficient miniaturized slot antenna [17]. In this paper, the CCLL-MTM structure is also utilized to miniaturize a slot antenna, however, it is shown that non-periodic double CCLL-MTM cells provide ε-negative (ENG) medium to miniaturize slot antennas with high gain and radiation efficiency. Moreover, this metamaterial structure exhibits a magneto-dielectric behavior at the higher frequencies, which helps to match the antenna through a broadband frequency range. At the higher frequencies, both the rectangular slot and CCLL-MTM cells resonate, which causes to increase the radiation gain and efficiency of the antenna while comparing with a simple printed rectangular slot. Although the MTM was known as a periodic structure, applying an element such as a unit-cell of MTM in antenna structures as a metamaterial-inspired antenna has been presented, and unusual properties of the MTM have been achieved [18]–[20]. The proposed antenna covers time-division-duplex LTE (TD-LTE) and a fraction of wireless local area network (WLAN) channels. The tangential electric field of resonating CCLL-MTM cells and the original slot are perpendiculars. Thus each band supports only a single horizontal/vertical polarization. The antenna is demonstrated experimentally. The simulation results are confirmed by measurements.

تاریخ دریافت: ۱۳۹۸/۰۲/۱۹ تاریخ پذیرش: ۱۳۹۸/۱۲/۰۱

2. ANTENNA CONFIGURATION

As described in the previous section, double cells of a CCLL-MTM structure have been used to achieve a miniaturized efficient high gain slot antenna. In this section, the constituent parameters of the cell are investigated.

2.1. Metamaterial Cell Design

Fig. 1 shows the simulated model of the MTM unit-cell. In order to retrieve the constituent parameters of the metamaterial cell, the aperiodic response is extracted by applying an electric field in the *xy*-plane, electric conductors (PEC) boundaries in the *yz*-plane, and a pair of perfect magnetic conductors (PMC) boundaries in the *xz*-plane. These boundaries usually set according to the directions of the electric and magnetic fields. To understand how to choose the electric and magnetic field vectors of Fig. 1(a), we have to study the fields' directions of the original slot antenna. The electric field of a rectangular slot antenna is illustrated in this figure. As shown later, the slot etched in the vicinity of the cell (Fig. 2). Thus, the E-field is set to be parallel with the CCLL-MTM surface while the H-field is perpendicular to the CCLL surface. The resultant scattering parameters obtained from CST microwave studio are exerted on Chen's algorithm [21]. The normalized impedance (z) and refractive index (n) of the model calculated as follows:

$$z = \pm\sqrt{\frac{(1+S_{11})^2 - {S_{21}}^2}{(1-S_{11})^2 - {S_{21}}^2}}, real(z) \geq 0$$
$$n = \frac{1}{k_0 d}\{[[\ln(e^{\acute{\imath}nk_0 d})] + 2m\pi] - i[\ln(e^{\acute{\imath}nk_0 d})]\} \quad (1)$$

where d is the MTM cell thickness and k_0 is the free space wave number and

$$Im(n) \geq 0, e^{ink_0 d} = \frac{S_{21}}{1 - S_{11}\frac{z-1}{z+1}} \quad (2)$$

The ambiguity of the value of m in (1) is resolved using Kramers-Kronig (KK) relating the real and imaginary parts of the index of refraction [22]

$$Re\big(n(\omega)\big) = 1 + \frac{2}{\pi} P.V.\left[\int_0^\infty \frac{\acute{\omega}\, Im\big(n(\acute{\omega})\big)}{\acute{\omega}^2 - \omega^2} d\acute{\omega}\right] \quad (3)$$

where $P.V.$ denotes the principal value of the integral and ω is the angular frequency. The effective permittivity (ε) and permeability (μ) of the medium can be expressed as $\varepsilon=n/z$, $\mu=nz$. Using FR4 as a dielectric material and the substrate thickness of 1.57 mm and a dielectric constant of ε_r=4.4, Fig. 1(b) shows the magnitude and phase components of S-parameters and retrieved effective ε/μ of the metamaterial cell.

It is evident that the CCLL-MTM unit-cell exhibits ENG behavior in the frequency range up to 3.5 GHz (Fig. 1(b)). According to this figure, at the lower frequencies the retrieved effective $|\varepsilon_r \times \mu_r|$ of the medium is high, which is preferred for antenna miniaturization. It exhibits a dispersive permittivity with the Drude model up to 3.5 GHz. Moreover, the effective medium shows magnetic behavior from f= 4.3 to 6 GHz where $\mu > 10$. The latest behavior helps to improve both impedance and radiation characteristics of the original slot antenna. The S-parameters and the resulted effective constitutive parameters are also confirmed by means of the Babinet principle as expected while comparing with CLL-MTM cell as described in [23].

Here, the effect of cell size on the effective permittivity of the cell is also investigated. The results are illustrated in Fig. 1(b)-right. It is assumed that the cell size reduced by 10% in the z-direction. It seems that the resulted effective permittivity changes drastically which affects the antenna miniaturization factor. The numerical simulations show that a change of –10% in c_{MTM} resulted to change the effective permittivity from –39 to –295.

2.2. Antenna Design

It is well-known that we can simply model an electrically small antenna (ESA) as a capacitor (C). When we load the antenna by an inductive element (L); its resonant frequency is approximately related to $f_r \propto \frac{1}{2\pi\sqrt{LC}}$. The CCLL-MTM behaves as this inductive element. Generally, MTM is known as a periodic structure that is realized by an infinite array of unit-cells. However, their anomalous properties have been observed when a single cell, metamaterial-inspired, structures have been employed to engineer a variety of small antennas. Here, it is shown that a non-periodic MTM structure, including a double asymmetrical CCLL-MTM structure, provides the required effective medium.

In this paper, first, we study a printed slot antenna. The antenna is designed to operate at 5.5 to 5.7 GHz. Next, by using a double asymmetrical CCLL cell, a metamaterial-inspired ENG medium is designed. The CCLL-MTM dimensions tuned to add an additional resonant frequency at 1900 MHz. Thus, the antenna design procedure contains two main steps:

a- Design printed slot antenna
b- Loading printed slot with CCLL-MTM cell to miniaturizing antenna

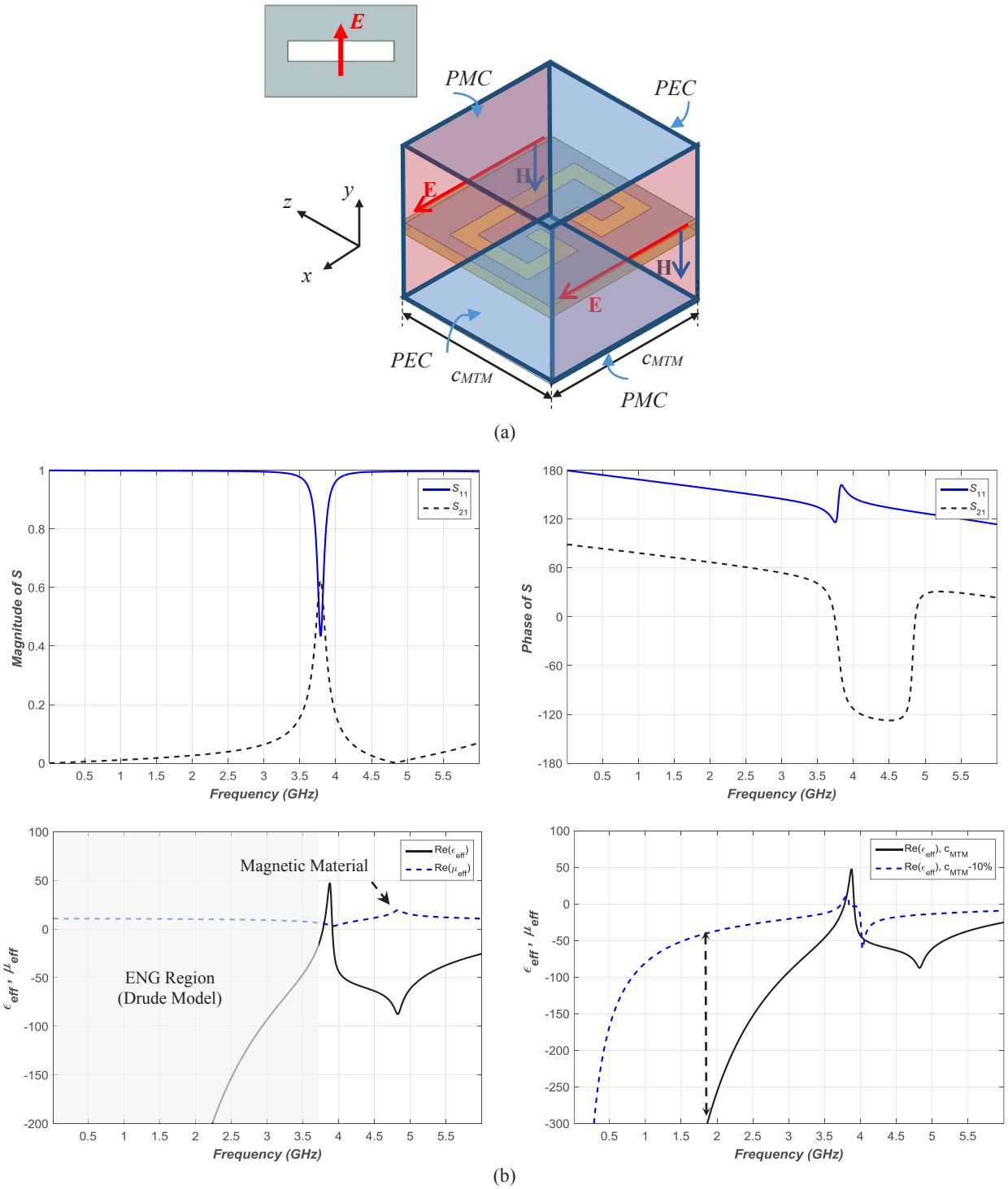

Fig. 1. Schematic of the CCLL-MTM cell and its design parameters: substrate thickness: h= 1.57mm, c_{MTM} = 23.625mm, substrate permittivity: ε_r=4.4, the cell parameters are labeled in Fig. 2, and (b) the retrieved effective parameters of the CCLL-MTM cell (left) and the effect of the cell size (right).

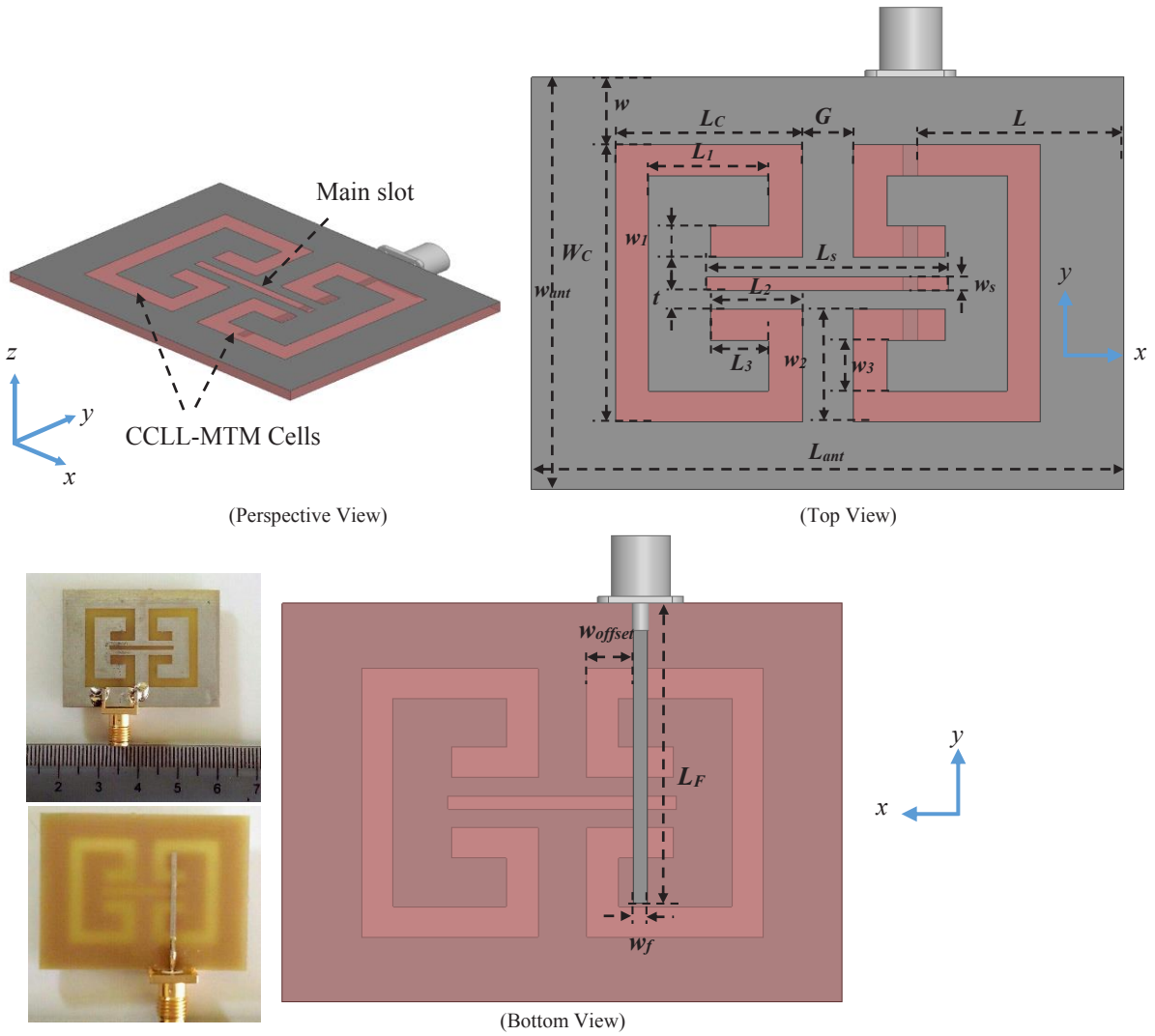

Fig. 2. Geometry of CCLL-MTM-loaded slot antenna: W_{ant}=29.4 mm, L_{ant}=39.2 mm, W_s=0.98 mm, L_s=16 mm, W_F=0.98 mm, L_F=22.15 mm, W_C=19.8 mm, L_C=12.37 mm, W=4.8 mm, L=13.65 mm, t=1.36 mm, G=3.4 mm, W_{offset}=3.27 mm, L_1=7.92 mm, L_2=6.06 mm, L_3=3.83 mm, w_1=2.22mm, w_2=8.04 mm, w_3=3.59 mm, and the manufactured prototype of the proposed antenna

The schematic of the CCLL-MTM–loaded slot antenna and the manufactured prototype are shown in Fig. 2. To increase the effectiveness and symmetry of the structure, two cells of CCLL-MTMs are etched in opposite directions on both sides of the slot. The CCLL-MTM cells are implemented in opposite directions to keep the assumed boundary condition of Fig. 1(a). The design parameters of the antenna and CCLL-MTM are also labeled in the figure caption.

The CCLL-MTM–loaded antenna is designed to work at the commercial handheld/portable frequency applications. LTE-TDD or TD-LTE is a 4G telecommunications technology. It is one of the two mobile data transmission technologies of the LTE technology standard, the other being frequency-division LTE (FD-LTE). There are two major differences between TD-LTE and FD-LTE: how data is uploaded and downloaded and what frequency spectra the networks are deployed in. While FD-LTE uses paired frequencies to upload and download data, TD-LTE uses a single frequency, alternating between uploading and downloading data through time. TD-LTE and FD-LTE also operate on different frequency bands. Frequencies used for TD-LTE range from 1850 MHz to 3800 MHz, with several different bands being used. The TD-LTE spectrum is generally cheaper to access and has less traffic. In this paper, the authors try to provide the TD-LTE-1900 MHz band using CCLL-MTM cell structure.

Here someone may say that the proposed structure is a simple combination of two folded long slots in the vicinity of a shorter one. In order to investigate whether an MTM cell exists or we only have three simple slots, a simple test procedure has been established here. For a simple resonator, the resonant frequency decreases by increasing the electrical size of the resonator. Moreover, it experiences a negligible variation by any change of the resonator location. It is due to the coupling effects which play critical roles in defining the

resonant frequency [24], and [25]. In contrast to a simple resonator, the resonant frequency corresponding to the effective medium which is provided by an MTM-cell has a remarkable variation by increasing the distance of the cell from the feed point location. In Fig. 3, the behavior of the loaded antenna as a function of a slot length, electrical size of the CCLL-MTM cell, and its location is investigated. As expected, increasing the electrical size of the slot and the CCLL-MTM cell leads to a decrease in their resonant frequencies. However, the lower resonant frequency is mainly attributed to the CCLL-MTM cell and the slot has less contribution (Fig. 3(a) and (b)). At first glance, it seems that we have three different resonators including a rectangular slot and the cells of CCLL-MTM. In order to clarify that we only have two simple resonators or an ENG metamaterial causes to miniaturize a slot antenna, we conduct an additional numerical simulation. According to Fig. 3(c), changing the feed line location causes considerable change at the low resonant frequency. Although the resulted resonant frequency occurred near the resonant frequency of a simple 68 mm resonator (1.88 GHz), the theory of a simple resonator could not explain this variation. Changing the feed line location leads to a change in the electric field distribution on the slot aperture. It consequently changes the effective size of the MTM cell and causes a drastic change of MTM behavior (as it demonstrated previously in Fig. 1(b)-right). The numerical simulations show that a change of about ±2% in c_{MTM} resulted to change the effective permittivity from −39 to −55. Thus the corresponding resonant frequency varies by the factor of $(1/\sqrt{39})/(1/\sqrt{55}) \cong 1.18$ which has good agreement with those obtained in this figure. Thus in contrary to the resonator physics, here we faced a metamaterial behavior.

3. SIMULATION AND TEST RESULTS

Fig. 4 shows the antenna impedance components and the simulated and measured s-parameters of the antenna with and without CCLL-MTM. As it seems in Fig. 4 (left), the presence of the CCLL-MTM loads causes a significant effect on the input impedance of the original slot antenna. Fig. 4 (right) compared the measured reflection coefficient of the antenna with the simulation results, with and without the CCLL-MTM loads. Good agreement between simulation and measurement results is obtained. The antenna designed to operate in portable handheld applications, thus the frequency bands extracted using $|S_{11}|<-6\ dB$.

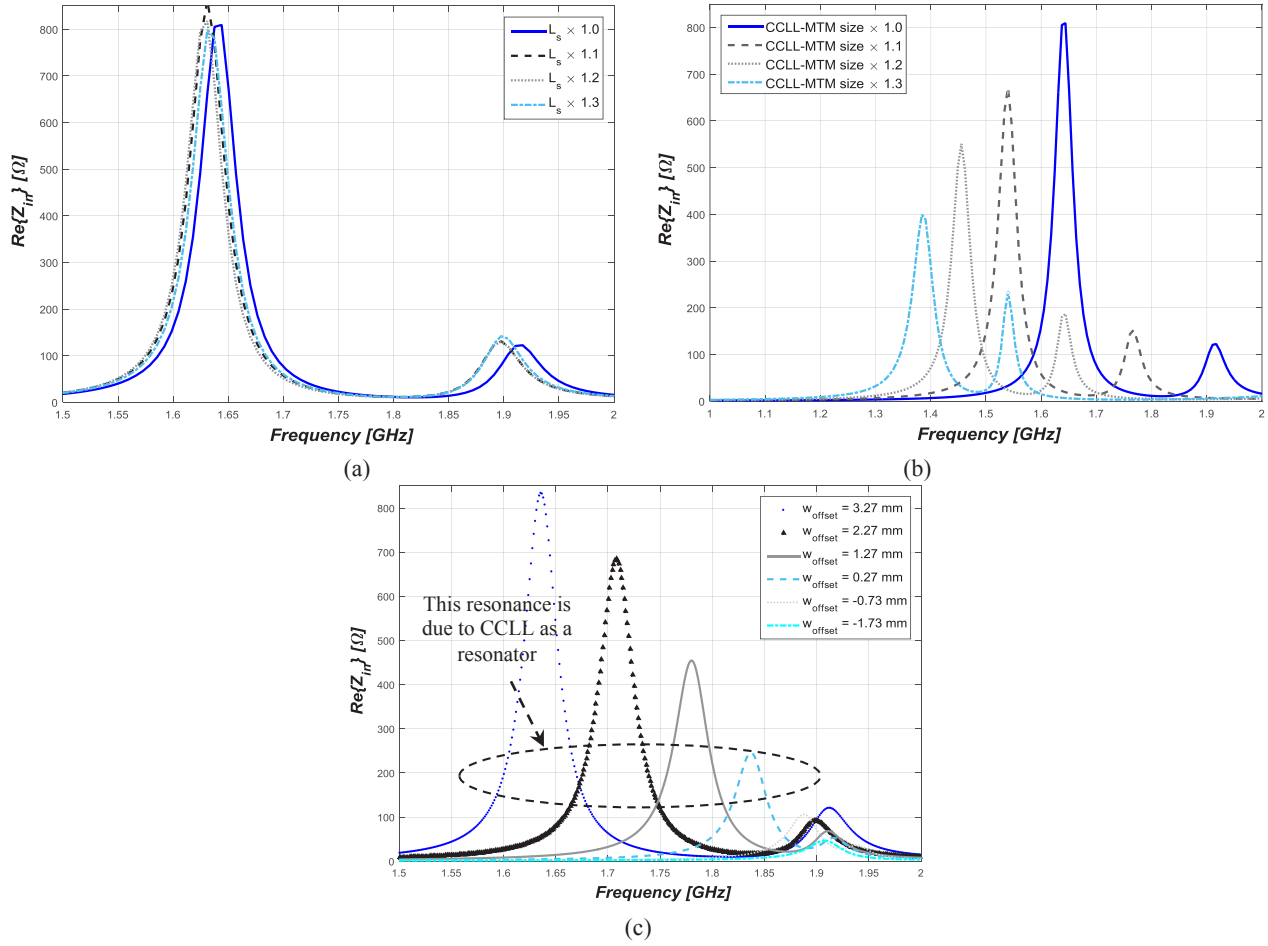

Fig. 3. Simulation results for the input impedance of the antenna versus (a) L_s, and (b) CCLL-MTM cell size, and (c) w_{offset}

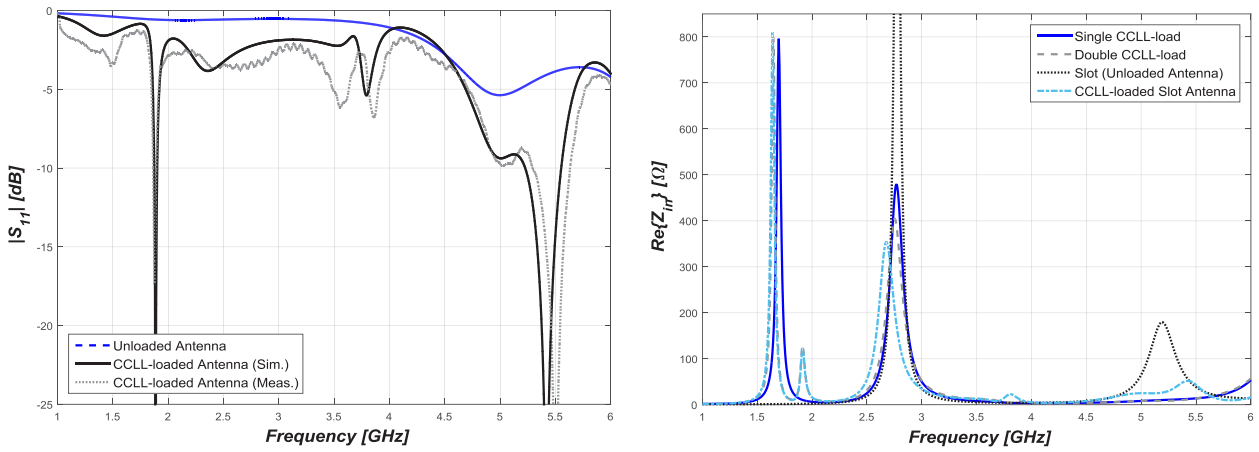

(a) (b)

Fig. 4. (a) Measured and simulated $|S_{11}|$ and (b) simulated real part of input impedance for unloaded and loaded slot antennas

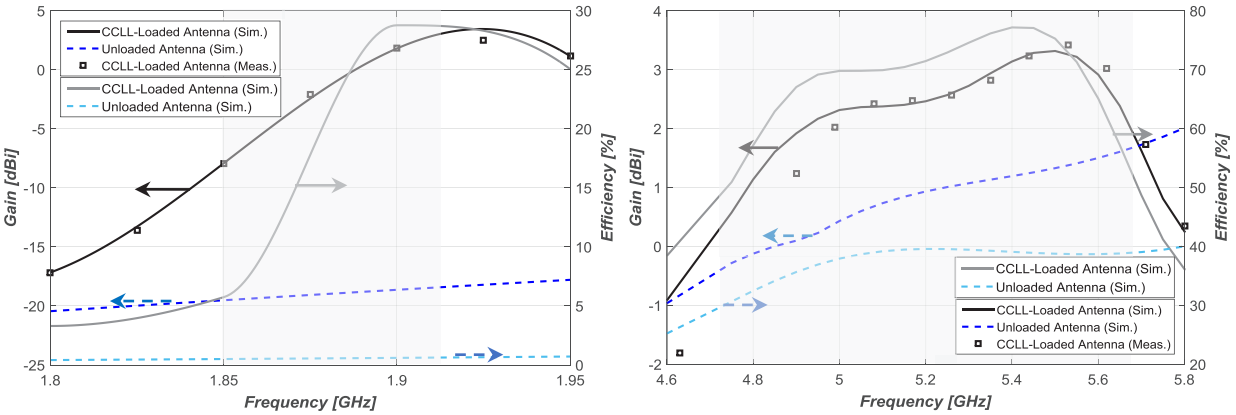

Fig. 5. Measured gain and simulated efficiency of loaded and unloaded antennas at the lower (left) and upper (right) frequency bands

The antenna shows a single band in a low-frequency regime that is tunable by changing the MTM cell size. Here, it is adjusted to cover PCS-1900 MHz and TD-LTE (1850–1910 MHz: the operating frequency of TD-LTE-1900 MHz (channel 35)). The ITU assigned the frequency band of 1850 to 1990 MHz to FD-LTE technology, however, the proposed antenna could not support both FD-LTE and TD-LTE simultaneously. The high-frequency band is expanded from 4750 to 5730 MHz. In the low-frequency band, the antenna impedance bandwidth of 3.2% from 1850 to 1910 MHz (60 MHz) is observed, while it is about 18.7% (980 MHz) in the higher band.

For an unloaded slot antenna printed on the same dielectric substrate (L_S = 16 mm), the resonant frequency is about 5.7 GHz. Comparing this resonance with that obtained in the proposed antenna, 1.9 GHz, more than 67% size reduction is achieved. The antenna has a dimension of $0.18\lambda_L \times 0.24\lambda_L \times 0.01\lambda_L$ (29.4×39.2 mm^2, f_L=1900 MHz, and λ_L is the free-space wavelength corresponding to the lower frequency).

Measured gain and simulated radiation efficiency of the antenna with (solid line) and without (dashed line) CCLL-MTM loads are compared in Fig. 5. As shown in this figure, the measured gain is almost close to those obtained by the simulation. However, the measured gain, especially in the higher band, does not agree well with the simulation. This discrepancy seems to be due to an enhanced perturbing effect on the antenna performance caused by the feeding structure, the cable, and the other practical issues.

The radiation efficiency of the antenna at the lower band frequencies is about 5 to 28% (with an average of 18%) along with -8dBi~2dBi gain (with the average of -2dBi). Although these values are low and they were not preferred in transceiver applications, they are acceptable while comparing with those obtained by the other metamaterial-based miniaturized antennas [4], [6], [8], and [10]. In the higher band, the radiation efficiency and antenna gain are in the range of 55~78% (with an average of 60%) and 0.5~3.5dBi, respectively.

At the lower frequencies, the unloaded antenna could not be matched and the antenna gain and efficiency are drastically lower than those obtained by the loaded antenna. Talking about the radiation performance, a fair comparison might be done with an unloaded slot antenna that resonating at the same frequency. Since, the main objective of this paper is to

investigate the effect of CCLL-MTM on a simple slot antenna, in this paper we compared an unloaded antenna with the loaded antenna that has the same overall dimensions. At the higher frequencies, both the rectangular slot and CCLL-MTM cells resonate simultaneously. It causes to increase the radiation gain and efficiency of the loaded antenna while compared with a simple unloaded slot antenna. On the other hand, the electrical size of the effective resonating slot at the higher frequencies is increased while utilizing a CCLL-MTM cell, which directly affected antenna radiation gain and efficiency.

Fig. 6 shows the distribution of the tangential component of the electric field of the CCLL-MTM–loaded slot antenna at f = 1.88 and 5.0 GHz. The antenna feed line is printed beneath the right cell. This asymmetrical geometry affected the electric field distribution, which causes radiation asymmetry at both lower and higher frequencies. According to this figure, at f = 1.88 GHz, there is an in-phase electric field distribution along the whole perimeter of the MTM unit-cell. The electric field has a significant component along the y-axis. The x-axis components canceled each other at the far-field. The coupled field strength at the MTM cells is not equal that consequently leads to a slightly more asymmetrical response of antenna radiation pattern at the lower band. At the upper-frequency band, both the rectangular slot and the CCLL-MTM cells resonate simultaneously. In contrary to the low frequencies, at the higher band, the electric field has a significant component along the x-axis. Due to the discrepancy of electric field directions, it is expected that two different types of polarizations be supported by the antenna at the lower and higher frequencies.

Measured far-field normalized radiation of the antenna is shown in Fig. 7(a) at f = 1.88, and 5.0 GHz. Due to the symmetry of the radiators, as like a conventional slot antenna, the radiation pattern is expected to be bi-directional. However, some slight asymmetry is attributed to the offset in the ground plane afforded by the physical SMA connector and feed line location. At the lower frequencies, comparable co- and cross-polarization components are obtained at both E- and H-planes. This feature is beneficial for handheld/portable devices since the position of them is non-predictable in practical applications. Since the size of the antenna (39.2 mm×29.4 mm) at the lower resonant frequency is about 0.24λ, as expected the radiation patterns are similar to an equivalent electric dipole, and a dipolar radiation pattern is achieved. Fig. 7(b) presents the polarization patterns of the antenna at f = 1.88, and 5.0 GHz. It is clear that the antenna shows different polarization behavior at these frequencies.

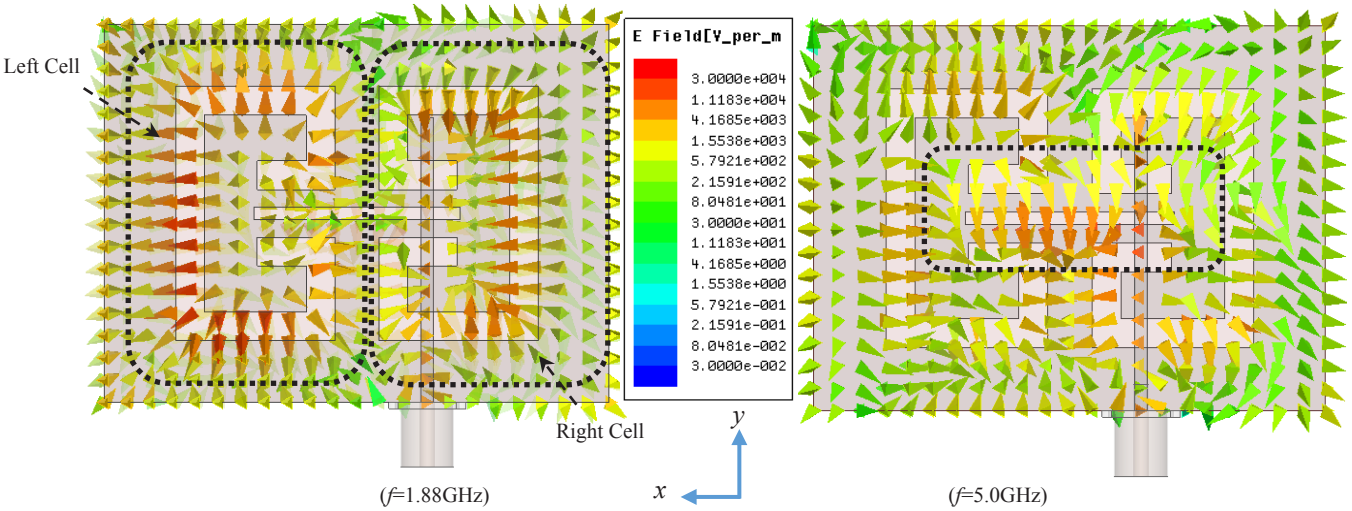

Fig. 6. Electric field distribution of the antenna.

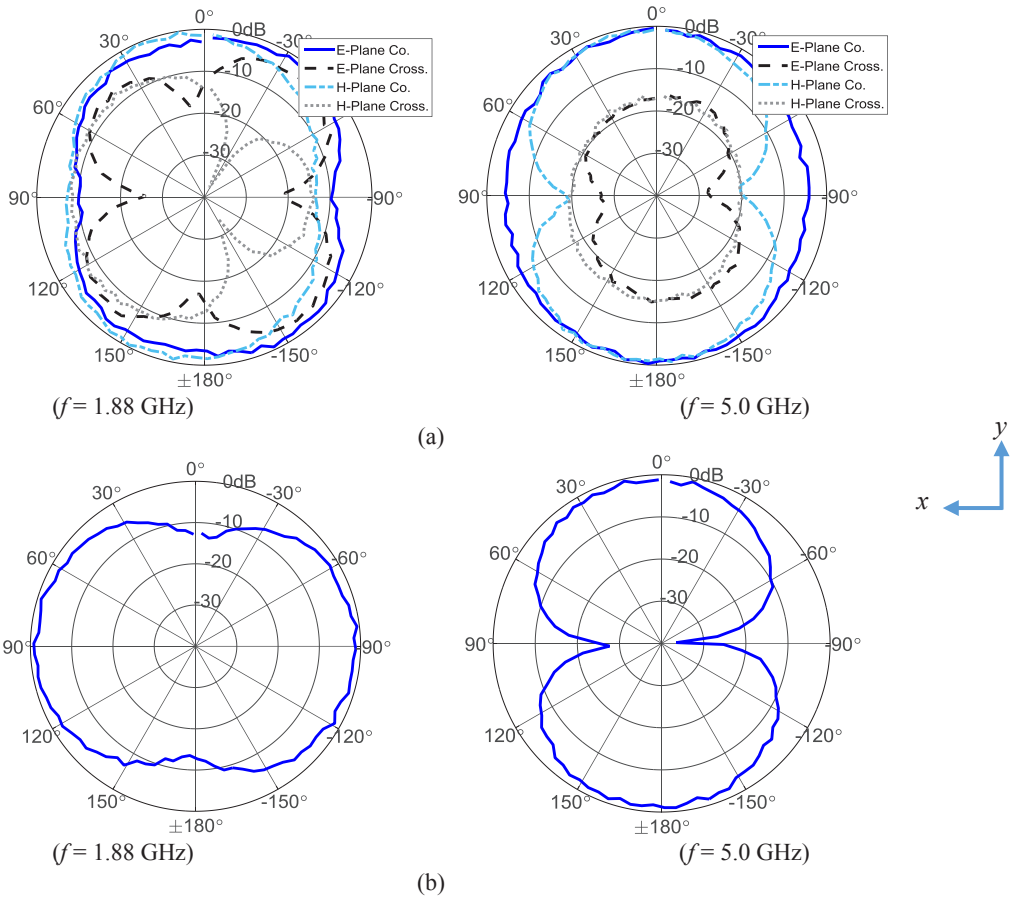

Fig. 7. (a) Measured normalized radiation and (b) simulated polarization patterns of the antenna at f=1.88, and 5.0 GHz.

4. CONCLUSION

A new planar compact dual-band dual-polarization antenna for handheld/portable applications has been presented. The antenna has a low profile, simple feed, moderate gain, and high efficiency over a broad operating frequency band. The antenna is comprised of three sections: a coupled-fed, two CCLL-MTM cells, and a slot. Utilizing CCLL-MTMs helped to obtain TD-LTE/WWAN, frequency bands. The antenna has a dimension of approximately $0.18\lambda_L \times 0.24\lambda_L \times 0.01\lambda_L$ (where λ_L is the wavelength corresponding to the antenna lower frequency) while achieving a peak gain and efficiency of 2/3.5 dBi and 28/78%, at the lower/higher band respectively.

REFERENCES

[1] M. M. Jacob, and D. F. Sievenpiper, "Gain and Noise Analysis of Non-Foster Matched Antennas," *IEEE Trans. Antennas Propagat*., Vol. 64, No. 12, pp. 4993–5004, 2016.

[2] N. Amani, A. Jafargholi, "Internal Uni-Planar Antenna for LTE/WWAN/GPS/GLONASS Applications in Tablet/Laptop Computers", *IEEE Antennas Wirel. Propag. Lett*., vol. 14, pp. 1654–1657, 2015.

[3] A Jafargholi, SA Akbarzadeh, MH Mazaheri, "Wideband microstrip patch antenna using ENZ metamaterials," *Microwave and Optical Technology Lett.* 56 (9), 2080-2084.

[4] N. Amani, A. Jafargholi, M. Kamyab, and A. Vaziri, "Asymmetrical wideband zeroth-order resonant antenna," *Electronics Lett*., vol. 50, no. 2, pp. 59-60, 2014.

[5] N. Amani, A. Jafargholi, "Zeroth-Order and TM_{10} Modes in One-Unit Cell CRLH Mushroom Resonator", *IEEE Antennas Wirel. Propag. Lett*., vol.14, 1396-1399, 2015.

[6] R. W. Ziolkowski, P. Jin, and C.-C. Lin, "Metamaterial-Inspired Engineering of Antennas," *IEEE Proceeding*, Oct. 2011.

[7] H. Mosallaei, and K. Sarabandi, "Design and Modeling of Patch Antenna Printed on Magneto-Dielectric Embedded-Circuit Metasubstrate" *IEEE Trans. Antennas Propag*., vol. 55, no. 1, 1031–1038, 2007.

[8] S. F. Mahmoud, "A new miniaturized annular ring patch resonator partially loaded by a metamaterial ring with negative permeability and permittivity," *IEEE Antennas Wireless Propag. Lett*., vol. 3, pp. 19–22, 2004.

[9] A. Alù, F. Bilotti, N. Engheta, and L. Vegni, "Subwavelength, Compact, Resonant Patch Antennas Loaded With Metamaterials," *IEEE Trans. Antennas Propag.*, vol. 55, no. 1, 13–25, 2007.

[10] N. Zhu, "Electrically small, near-field resonant parasitic (NFRP) antennas augmented with passive and active circuit elements to enhance their functionality," *Ph.D. Thesis*, *University of Arizona* 2013.

[11] A. Erentok, P. Luljak, and R. W. Ziolkowski, "Antenna performance near a volumetric metamaterial realization of an artificial magnetic conductor," *IEEE Trans. Antennas Propagat.*, vol. 53, pp. 160–172, 2005.

[12] A. Jafargholi, M. Kamyab, and M. Veysi, "Artificial magnetic conductor loaded monopole antenna," *IEEE Antennas Wireless Propag. Lett.,* vol. 9, pp. 211–214, 2010.

[13] A. Jafargholi, and M. Mohammadkhani, "Miniaturized Microstrip Antenna Using High Impedance Wires Incorporating AMC MTMs," *Int. J. Electronics Lett*., vol. 4, no. 4, pp. 489–496, 2016.

[14] A. Jafargholi, M. Kamyab, M. Rafaei Booket, and M. Veysi, "A compact dual-band printed dipole antenna loaded with CLL-based metamaterials" *Int. Rev. Electrical Engineering*, vol. 5, no. 6, 2010.

[15] A. Jafargholi, A. Jafargholi, and J. H. Choi, "Mutual Coupling Reduction in an Array of Patch Antennas Using CLL Metamaterial Superstrate for MIMO Applications," *IEEE Trans. Antennas Propagat*., vol. 67, no. 1, pp. 179-189, 2019.

[16] A. Jafargholi, A. Jafargholi, J. H. Choi, M. Veysi, A. Soleimani, "Microstrip Patch Back Radiation Reduction Using Metamaterial Superstrate," *IET Microwave Antenna Propag*., vol. 14, no. 2, pp. 158-164, 2020.

[17] A. Jafargholi, and A. Jafargholi, "Miniaturization of Printed Slot Antennas Using Artificial Magnetic Conductors," *IET Microwave Antenna Propag*., vol. 12, no. 7, 2018.

[18] A. Erentok and R. W. Ziolkowski, "Metamaterial-inspired efficient electrically-small antenna," *IEEE Trans. Antennas Propag*., vol. 56, no. 3, 691–707, Mar. 2008.

[19] M. Rafaei Booket, A. Jafargholi, M. Kamyab, H. Eskandari, M. Veysi, and S. M. Mousavi, "A Compact Multi-Band Printed Dipole Antenna Loaded with Single-Cell MTM," *IET Microwave Antenna Propag*., Vol. 6, No. 1, pp. 17-23, 2012.

[20] N. Amani, M. Kamyab, A. Jafargholi, A. Hosseinbeig, and J. S. Meiguni, "Compact tri-band metamaterial-inspired antenna based on CRLH resonant structures," *Electronics Lett*., vol. 50, no. 12, pp. 847-848, 2014.

[21] X. Chen, T. M. Grzegorczyk, B. I. Wu, J. Pacheco, J. A. Kong, "Robust method to retrieve the constitutive effective parameters of metamaterials", *Phys. Rev. E* 70, 016608 (2004)

[22] Z. Szabó, G. H. Park, R. Hedge, and E. P. Li, "A Unique Extraction of Metamaterial Parameters Based on Kramers–Kronig Relationship," *IEEE Trans. Microwave Theory Tech*., vol. 58, no. 10, 2646-2653, 2010.

[23] F. Falcone, T. Lopetegi, A. G. Laso, J. D. Baena, J. Bonache, M. Beruete, R. Marque´s, F. Martin, and M. Sorolla, "Babinet Principle Applied to the Design of Metasurfaces and Metamaterials," *Physical Review Letters*, vol 93, No. 19, 197401, 2004.

[24] C. C. Lin, P. Jin, and R. W. Ziolkowski, "Single, Dual and Tri-Band-Notched Ultrawideband (UWB) Antennas Using Capacitively Loaded Loop (CLL) Resonators," *IEEE Trans. Antennas Propag*., vol. 60, no. 1, pp. 102–109, 2012.

[25] M. Rafaei Booket; M. Veysi; Z. Atlasbaf; A. Jafargholi, "Ungrounded Composite Right/Left Handed Metamaterials: Design, Synthesis, and Applications," *IET Microwave Antenna Propag*., Vol. 6, No. 11, pp. 1259-1268, 2012.